Performance Comparison of Modified BPSK-OFDM and QFSK-OFDM in PLC Channel Noise

Abiola G. Bolaji, and Thokozani Shongwe

Abstract—The article describes and compares two OFDM based communications schemes for reducing the effects of the combination of Narrowband Interference (NBI) and Impulsive Noise (IN), which are noise types typical in Power Line Communication (PLC). The two schemes are *Modified* BPSK-OFDM (called MBPSK, for brevity) and QFSK-OFDM (called QFSK, for brevity), which are non-conventional OFDM schemes. We give a description of the two schemes, showing how they are derived and also show their similarities and eventually compare their performances. Performance simulation results, in terms of bit error rate, are given to compare the systems under the effect of IN and NBI. The popular Middleton Class A model is used for modelling IN. The results show that MBPSK scheme outperforms the QFSK scheme in terms of minimum distance, and hence in terms of bit error probability when no preprocessing is performed. However, under clipping/nulling, both schemes eventually reach the bit error rate floor.

Keywords—narrow-band Interference, impulsive noise, power-line communications, BPSK-OFDM, QFSK-OFDM

I. INTRODUCTION

PLC is a technology that aims at reusing the existing power lines, for which were primarily meant for the delivery of AC/DC electric power, for the purposes of data transmission [1]. Unfortunately, the PLC channel has shown to be a very harsh and noisy environment for the data. It has time-variant characteristics as a result the PLC channel is difficult to model. This makes the channel to stand out from other communication mediums found in other communication systems. For example, it is susceptible to a mixture of the noise types, Impulsive Noise (IN), Narrowband Interference (NBI) and Additive White Gaussian Noise (AWGN) whilst in other systems AWGN can be used to describe the noise experienced by the channel. The noise challenge in PLC has inspired researchers in the communications community to find means of making the PLC channel more realiable for data transmission. This has resulted into finding ways to mitigate the effect of the aforementioned noises. Lately Coded Modulation has been viewed as another way to reduce the effect of noise on the transmitted data, besides threshold-dependent methods, error correction codes, to name but a few [2], [3], [4], [5], [6].

Initially, IN has got much attention for it has been viewed as the most destructive noise and it is experienced across most communications systems, with NBI coming as the second destructive noise. This has resulted to have research done extensively on the individual effect of each noise (IN plus AWGN or NBI plus AWGN) and not as a combination of all three. Some techniques have been proposed by various researchers. For instance, Sanjana and Suma based on the threshold-based techniques (clipping and nulling) for IN in the time domain and frequency suppression for NBI in frequency domain [7]. In [8] an iterative approach is proposed based on the use of multiple-signal characterizing (MUSIC) method, least square (LS) estimator and minimum mean square error (MMSE) estimator whilst [9] proposes a method aligned to coded modulation where he used a conventional modulation scheme and permutation codes. Part of the work contributed in [10] shows the better performance of MBPSK scheme under the influence of different system parameters when compared to the QFSK scheme. These schemes both fall under means of using coded modulation to mitigate both NBI and IN.

In this paper, we develop our work from [10] by using hybrid modulated systems to mitigate the joint effect of IN and NBI. We further provide analysis and the short comings of each presented method (i.e modified BPSK-OFDM and QFSK-OFDM). For brevity, conventional BPSK-OFDM as CBPSK, QFSK-OFDM and modified BPSK-OFDM shall be referred to as QFSK and MBPSK, respectively. Then the rest of the paper is structured as follows: Section II briefly describes the system model used for simulations, Section III will mathematically outline the modulation schemes proposed, Section IV is on the simulation and analysis of the results based on the Bit Error Rate curves of each modulation scheme. Lastly, will be the conclusion V.

A. G. Bolaji is with Department of Electrical and Electronic Engineering Science, University of Johannesburg, Johannesburg, South Africa (e-mail: adukebolaji@ymail.com).
T. Shongwe is with Department of Electrical and Electronic Engineering Technology, University of Johannesburg, Johannesburg, South Africa (e-mail: tshongwe@uj.ac.za).

II. SYSTEM MODEL

The communication system model used in this work is shown in Figure 1. With reference to this Figure 1, the modulation block receives a stream of N bits, where $\mathbf{I} = [b_1, b_2, \ldots, b_N]$, $b_i \in \{0, 1\}$ and, '0' and '1' have been randomly generated with equal probability. Within the modulation section, the bits are mapped into x-tuples which go through either QFSK or MBPSK modulation. This results to Z vector blocks of length M, denoted by S_l, whereby each element of S_l is a symbol as per the specific modulation used. As a result, the whole transmitted message will be of total length $L = MZ$. The M represents the number of frequencies used for transmission which is equal to the length of each block. Each vector block S_l is made up M symbols. The transmitted message can be presented in a $Z \times M$ matrix as follows

$$\mathbf{S} = \begin{bmatrix} S_1 \\ S_2 \\ \vdots \\ S_Z \end{bmatrix} = \begin{bmatrix} a_{11} & a_{12} & \ldots & a_{1M} \\ a_{21} & a_{22} & \ldots & a_{2M} \\ \vdots & \vdots & \vdots & \ddots \\ a_{Z1} & a_{Z2} & \ldots & a_{ZM} \end{bmatrix}. \quad (1)$$

The overall mapping of the x-tuples from I to M elements in S_l is the *Coded Modulation* MBPSK-OFDM or QFSK-OFDM as,

$$\begin{array}{ccccccc} b_1 & b_2 & \longrightarrow & a_{11} & a_{12} & \ldots & a_{1M} \\ b_3 & b_4 & \longrightarrow & a_{21} & a_{22} & \ldots & a_{2M} \\ \vdots & \vdots & \vdots & \vdots & \vdots & \vdots & \vdots \\ b_{N-1} & b_N & \longrightarrow & a_{Z1} & a_{Z2} & \ldots & a_{ZM}. \end{array} \quad (2)$$

The binary x-tuple is information bits that indicate the position of the unique symbol '1' per block as seen in Figures 2 and 3. These proposed modulation schemes, MBPSK and QFSK have a condition of uniquely assigning the symbol '1' per block of $M = 4$ sub-carries, and then assigning symbol '0' (QFSK) or '−1' (MBPSK) in the rest of the $M - 1$ sub-carriers in the block as illustrated in Figures 2 and 3, creating vector blocks of length $M = 4$ as indicated by the rows of the matrix in (1). Each vector block is then translated into the corresponding time domain block, s_l via the Inverse Fast Fourier Transform as

$$s_l(v) = \frac{1}{\sqrt{M}} \sum_{k=0}^{M-1} S_l(k) e^{j2\pi vk/M} \quad (3)$$
$$v = 0, 1 \ldots M - 1, l = 1, 2, \ldots, Z,$$

where $S_l(k)$ is the kth element of the lth vector block defined as $S_l(k) = a_{lk}$ in the matrix in (1). The time domain block s_l is transmitted through the PLC channel which is subject to IN, NBI, and AWGN. Therefore, the corrupted received signal in vector block form, r_l can be expressed as

$$r_l = s_l + F_l + \Theta_l + \Upsilon_l, \quad l = 1, 2, \ldots, Z, \quad (4)$$

where F_l, Θ_l, Υ_l are the lth vector block of Narrowband Interference, Impulsive noise, AWGN in time domain where the vector blocks are of the length M which corresponds to the length of s_l.

A. Brief Noise Models Overview

To model the major noise types, the popular 2-state model Middleton Class A model is used for IN as described in [11]. The Probability Density Function (PDF) is expressed as zero-mean Gaussian terms weighted by a Poisson distribution process,

$$p_{in}\left[\bar{\Theta}_l(k)\right] = \sum_{m=0}^{\infty} \frac{e^{-A}A^m}{m!} \frac{1}{\sqrt{2\pi\sigma_m^2}} e^{\frac{-\bar{\Theta}_l(k)^2}{2\sigma_m^2}},$$

where $\bar{\Theta}_l(k)$ is the kth element in the lth IN vector, σ_m^2 is the variance in the system, A is the impulsive index, which is the measure of the IN impulsiveness, m is the possible number of IN to be observed within a certain period. The A parameter is well explained in [11]. The overall variance can be expressed as

$$\sigma_m^2 = \sigma_i^2 \frac{m}{A} + \sigma_g^2$$
$$= \sigma_i^2 \frac{\frac{m}{A} + \Gamma}{1 + \Gamma},$$

for $\Gamma = \frac{\sigma_g^2}{\sigma_i^2}$ is the AWGN to IN power ratio, where $m = 1, 2, \ldots \infty$, σ_g^2 is the AWGN variance and σ_i^2 is the IN variance. The probability of IN occurring, Λ, is taken as the $A \therefore \Lambda = A$.

The NBI model used is similar to the Middleton Class A model as used for IN, as taken from [12]. According to Shongwe *et. al* [12], the NBI amplitudes in the frequency domain are also assumed to be Gaussian variables with a zero-mean, with chances of occurrence treated as a Poisson process. Therefore, the PDF is expressed as

$$p_{nbi}\left[\bar{F}_l(k)\right] = \sum_{m=0}^{\infty} \frac{e^{-\lambda}\lambda^m}{m!} \frac{1}{\sqrt{2\pi\sigma_m^2}} e^{\frac{-\bar{F}_l(k)^2}{2\sigma_m^2}},$$

where $\bar{F}_l(k)$ is the kth element in the lth NBI vector, $\sigma_m^2 = m\sigma_{nbi}^2/\lambda$ is variance, m is the possible number of NBI, λ is the fraction of frequency the interference occupies in the system of bandwidth W. λ is analogous to A so it is treated as the probability of NBI occurring.

The simulation of the NBI model is governed by the function

$$\bar{F}_l(k) = \sqrt{\mu} + \sqrt{\bar{\chi}}R_g,$$

where the $\mu = 0$, $\bar{\chi} = \sigma_{nbi}^2/\lambda$ is the average power of NBI expected to be contributed by a single interference, and R_g is the random function based on the standard normal distribution. σ_{nbi}^2 is the total average effective NBI power within the whole system. In all the levels of the presented simulation, the parameters: Γ, A, λ, σ_{nbi}^2, σ_i^2 are kept constant. On that
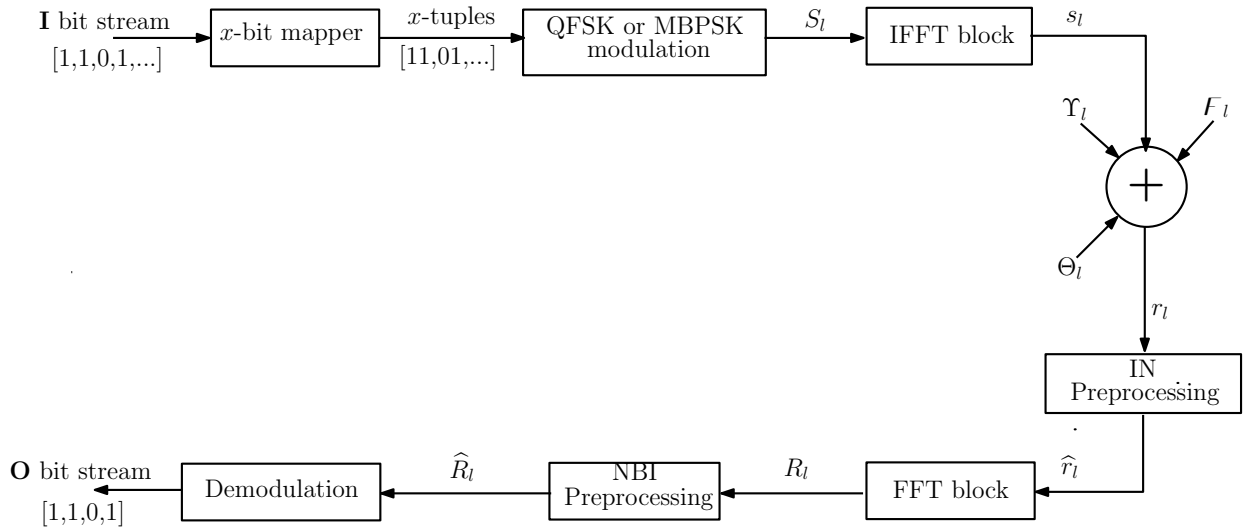
Fig. 1. The OFDM-based PLC system block diagram with non-linear preprocessor for IN and NBI respectively before the demodulator.
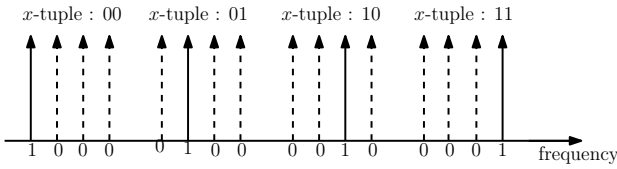

Fig. 2. OFDM sub-carriers grouped into blocks of $M = 4$. An x-tuple is mapped onto a size M QFSK vector block, such that a symbol '1' is assigned to one sub-carrier in a group of M sub-carriers as indicated by a solid line. The rest of the $M - 1$ sub-carriers are assigned symbol '0' as indicated by the dotted lines. Here $x = \log_2(M) = 2$.
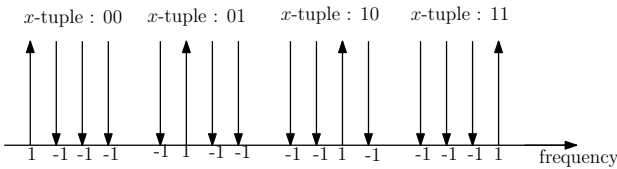

Fig. 3. OFDM sub-carriers grouped into blocks of $M = 4$. An x-tuple is mapped onto a size M MBPSK vector block, such that a symbol '1' is assigned to one sub-carrier in a group of M sub-carriers as indicated by a solid line. The rest of the $M - 1$ sub-carriers are assigned symbol '−1' as indicated by the up–side down lines. Here $x = \log_2(M) = 2$.

account, the work to be presented, the signal-to-noise ratio (SNR) in decibels is as follows

$$SNR_{dB} = 10 \log_{10}\left(\frac{E_b}{N_g + N_i + N_{nbi}}\right)$$
$$= 10 \log_{10}\left(\frac{E_b}{K}\right). \tag{5}$$

For generality, let N_n be the two-sided noise power spectral density for noise type n, corresponding to noise variance σ_n^2. Such that N_g, N_i, and N_{nbi} are the two-sided noise power spectral densities for Gaussian noise (AWGN), Impulse noise and Narrowband Interference, respectively.

B. Noise Mitigation Measures

The received signal matrix is taken through the non-linear preprocessor to either null or clip the signal detected as corrupted. As shown in Figure 1, there are two processing blocks, one implemented in the time domain and the other frequency domain, one for each noise type (IN or NBI). The received signal is only processed when its amplitude exceeds a set threshold and then goes to the block demodulator, which gives out a bit stream **O**.

The IN corrupted symbols are identified by a threshold before being translated to the frequency domain where NBI corrupted symbols are identified by threshold before the decision making level in the demodulation functional block. The IN preprocessing block is governed by

$$\widehat{r}_l(k) = \begin{cases} r_l(k) & , & |r_l(k)| \leq T_{in} \\ r_l(k) \times X & , & |r_l(k)| > T_{in}, \end{cases}$$

where $\widehat{r}_l(k)$ is the result of clipping in time domain and $X \geq 0$. When $X = 0$ is a special case of clipping called nulling.

Then after the FFT, the mitigation of NBI is performed, whereby the NBI preprocessing block is governed by

$$\widehat{R}_l(k) = \begin{cases} R_l(k) & , & |R_l(k)| \leq T_{nbi} \\ \sqrt{E_b} \times X & , & |R_l(k)| > T_{nbi}, \end{cases}$$

where $\sqrt{E_b}$ is the linear signal amplitude, $R_l(k)$ is the result of clipping the kth element of the R_l vector block in frequency domain, and $R_l = [b_{l1}, b_{l2}, \ldots, b_{lM}]$ as the noise corrupted version of S_l after it has gone through the channel and $X \geq 0$ and $l = 0, 1, \ldots, Z - 1$.

III. MATHEMATICAL SYSTEM AND MODULATION DESCRIPTION

The use of 2-tuples, and blocks of size M leads to the system producing a codebook C, of M-element row vectors such that the ith codeword can be represented as $C_i = [c_1^i \ c_2^i \ \dots \ c_M^i]$. This C_i corresponds to the transmitted block S_l. For the coded modulation QFSK-OFDM, where $M = 4$ the codewords of the codebook C^q are

$$
\begin{aligned}
C_1 &= \begin{bmatrix} 1 & 0 & 0 & 0 \end{bmatrix} \\
C_2 &= \begin{bmatrix} 0 & 1 & 0 & 0 \end{bmatrix} \\
C_3 &= \begin{bmatrix} 0 & 0 & 1 & 0 \end{bmatrix} \\
C_4 &= \begin{bmatrix} 0 & 0 & 0 & 1 \end{bmatrix},
\end{aligned} \quad (6)
$$

such that a row in C^q codebook is a codeword C_i, for $1 \le i \le M$.

For the case of MBPSK, where also $M = 4$ the codewords of the codebook, C^m is generated as

$$
\begin{aligned}
C_1 &= \begin{bmatrix} 1 & -1 & -1 & -1 \end{bmatrix} \\
C_2 &= \begin{bmatrix} -1 & 1 & -1 & -1 \end{bmatrix} \\
C_3 &= \begin{bmatrix} -1 & -1 & 1 & -1 \end{bmatrix} \\
C_4 &= \begin{bmatrix} -1 & -1 & -1 & 1 \end{bmatrix},
\end{aligned} \quad (7)
$$

such that a row in C^m codebook is a codeword C_i, for $1 \le i \le M$.

MBPSK is basically a coded version of conventional BPSK-OFDM in the sense that MBPSK restricts its choice of codewords sequences of length $M = 4$ to just four as shown in (7), whilst BPSK-OFDM has no restriction. These two modulation schemes can be compared in terms of distances and data rate.
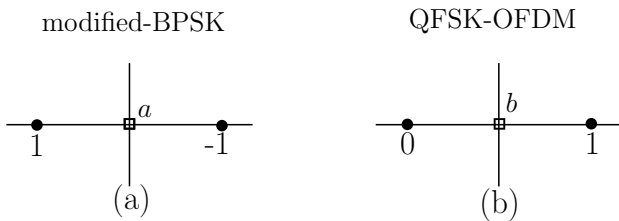
modified-BPSK   QFSK-OFDM

Fig. 4. The constellation of MBPSK and QFSK on a 2-dimensional plane.

1) Distance metrics: The uniquely assigning of symbol '1' is clearly demonstrated in Figures 2 and 3, and further by the codebooks of the respective modulation schemes in (6) and (7). In the case of QFSK, only one sub-carrier will be expected to have the signal power with the $M - 1$ sub-carriers acting as dummy sub-carriers. For MBPSK, the one sub-carrier will have a positive phase, whilst the rest will have a negative phase. The solid lines signify that the sub-carrier has the signal power, whilst the dashed line signifies that the sub-carrier has no power. The downward

pointing arrows signify the opposite phase of the signal found in that sub-carrier.

Furthermore, when considering the constellation of each scheme as shown in Figure 4, the Euclidean distance squared d^2 between the elements, c_1^i and any other element c_M^i is different for each scheme. The Euclidean distance squared is the system's measure on its robustness in withstanding AWGN. QFSK has $d^2 = 1$, while MBPSK has $d^2 = 2$. This means that MBPSK will perform better than QFSK under AWGN, since it has twice the d^2 of QFSK.

2) Modulation Rates: Having vector blocks of size M generated from a set $\{0, 1\}$ will produce 2^M codewords sequences of length M. When $M = 4$, that means there will be 16 codewords sequences of length four. Recall that the modulation schemes proposed takes x-tuple sequences from **I** and map them to codewords C_i. Therefore for $x = 2$ the codewords sequences of length $M = 4$ are reduced from 16 to 4 codewords. Instead of using or transmitting from the whole of 2^M set sequences, MBPSK and QFSK restricts the choice of sequences to 4. Concerning the code rate in terms of information bits and redundancy bits, the code rate $R_c = 1/2$ for both modulation schemes. Without any form of coded modulation, the code rate stays at 1 as it is the case in conventional BPSK-OFDM. As a result, conventional BPSK-OFDM is said to be spectral efficient than both MBPSK and QFSK.

3) Mathematical Transform Effect: The choice of transform used to move from one domain to another in this paper plays a role in the behaviour of the proposed schemes. The chosen Fourier Transform involves a defined Discrete Fourier Transform (DFT) matrix, **Y**, which is dependent on the number of sub-carriers considered also called the length of the FFT, which is M in our case [13]. To demonstrate, let

$$
\mathbf{Y} = \begin{bmatrix}
1 & 1 & \dots & 1 \\
1 & A & \dots & A^{2(M-1)} \\
\vdots & \vdots & \dots & \vdots \\
1 & A^{2(M-1)} & \dots & A^{(M-1)(M-1)}
\end{bmatrix}, \quad (8)
$$

for $A[l, v] = e^{-j2\pi vl/M}$, $v = 0, 1, 2, \dots, (M-1)$, $l = 0, 1, \dots, Z - 1$. By knowing the number of sub-carriers that will be used gives one the ability to calculate **Y**. For $M = 4$, the Inverse Fast Fourier Transform (IFFT) matrix, $\widetilde{\mathbf{Y}}$, is the transpose of **Y** as the time domain matrix and **Y** can be expressed as

$$
\mathbf{Y}(4) = \begin{bmatrix}
1 & 1 & 1 & 1 \\
1 & -j & -1 & j \\
1 & -1 & 1 & -1 \\
1 & j & -1 & -j
\end{bmatrix}, \quad (9)
$$

and

$$\widetilde{\mathbf{Y}}(4) = \begin{bmatrix} 1 & 1 & 1 & 1 \\ 1 & j & -1 & -j \\ 1 & -1 & 1 & -1 \\ 1 & -j & -1 & j \end{bmatrix}. \tag{10}$$

Taking a QFSK vector, for example, $S_l^q = [1 \ 0 \ 0 \ 0]$, and translating it to the time domain, it can be expressed as

$$s_l^q = S_l^q \times \frac{\widetilde{\mathbf{Y}}(M)}{\sqrt{M}} \tag{11}$$
$$= [0.5 \ 0.5 \ 0.5 \ 0.5],$$

where the transform is normalised by $\sqrt{M}$.

Also taking a MBPSK vector, for example, $S_l^m = [1 \ -1 \ -1 \ -1]$ and translating it to the time domain can be expressed as

$$s_l^m = S_l^m \times \frac{\widetilde{\mathbf{Y}}(M)}{\sqrt{M}} \tag{12}$$
$$= [-1 \ 1 \ 1 \ 1],$$

where the transform is normalised by $\sqrt{M}$.

The results for (11) and (12) demonstrate a scenario where the first sub-carrier of the lth block has symbol '1'. Using $S_l^q = [1 \ 0 \ 0 \ 0]$ which equals to C_1 for QFSK, implies that the first row in the matrix in (10) will be useful in the transform and all other rows will be summed up as zeroes. If the symbol '1' is inserted in the second sub-carrier, $[0 \ 1 \ 0 \ 0]$, then the 2nd column will be used in the transform, and so on. On the other hand, for MBPSK the rows without the symbol '1' are considered by the transform since the amplitude of each element in the row affects the summing up of the sinusoids in (8). The time domain symbols, s_l^m and s_l^q demonstrate that MBPSK has a way of preserving the signal amplitude. By assuming the symbols to be in a 4-dimensional plane and taking each symbol a point on the plane, the Euclidean distance within the codebook C^m is higher than that of codewords in C^q.

IV. SIMULATION RESULTS AND ANALYSIS

This section focuses on the performance of QFSK scheme in comparison to MBPSK scheme based on the BER curves, probability of failure and probability density function threshold curves. Throughout the investigation as to which noise could be destructive between IN and NBI when considered as mixture, NBI worsened the system's performance. Recall, that IN is an amplification of AWGN which occurs with a certain probability in the time domain whilst in the frequency domain it spreads on the sub-carriers thus affecting the transmitted

signal with diminished power depending on the size of the FFT. On the other hand, NBI is prominent in the frequency domain as is the transmitted signal. That is to say, the block S_l's behaviour is the same as that of NBI block F_l, in the frequency domain. Therefore, NBI has the potential to significantly decrease or increase the amplitude of the desired signal if it is in the same sub-carrier as the signal. This makes NBI a concern since dealing with it can affect the signal.
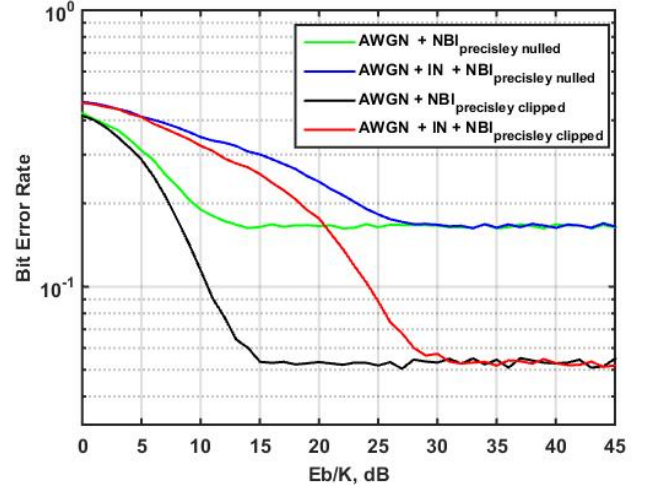

Fig. 5. The QFSK scheme in cases of clipping and nulling NBI at perfect noise locations, where $\Lambda = \lambda = 0.25$, $\sigma_{nbi}^2 = 100$, $\Gamma = 0.1$, and $X = 0.5$.
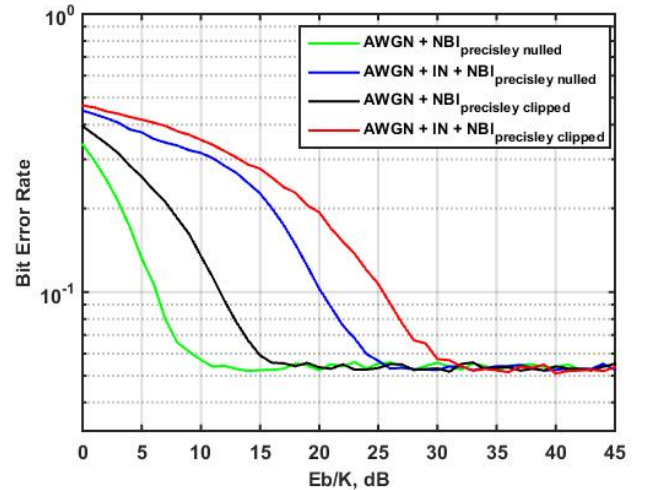

Fig. 6. The MBPSK scheme in cases of clipping and nulling NBI at perfect noise locations, where $\Lambda = \lambda = 0.25$, $\sigma_{nbi}^2 = 100$, $\Gamma = 0.1$, and $X = 0$.

We will look at the mitigation of NBI in the NBI preprocessing block where the perfect knowledge of NBI location technique is used. To combat NBI, the NBI is identified and either clipped or nulled in the 'NBI preprocessing block' in Figure 1. To evaluate the effect of NBI preprocessing, we begin by providing the bounds of good system performance, where
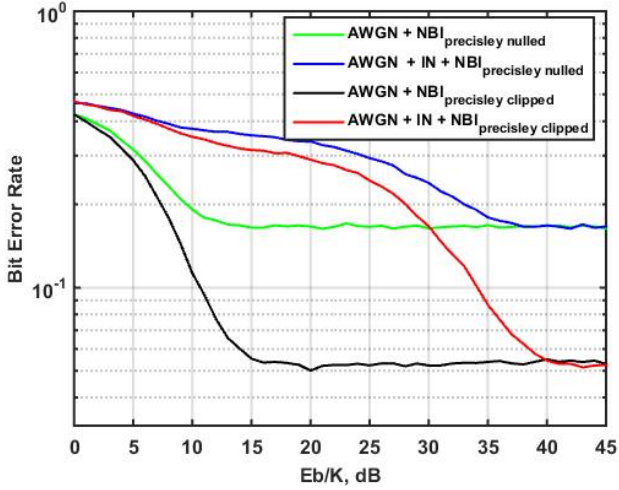
Fig. 7. The QFSK scheme in cases of clipping and nulling NBI at perfect noise locations, where $\Lambda = \lambda = 0.25$, $\sigma_{nbi}^2 = 100$, $\Gamma = 0.01$, and $X = 0.5$.
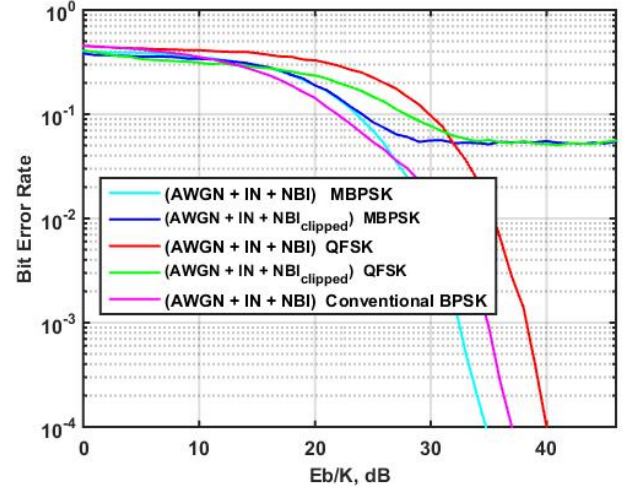

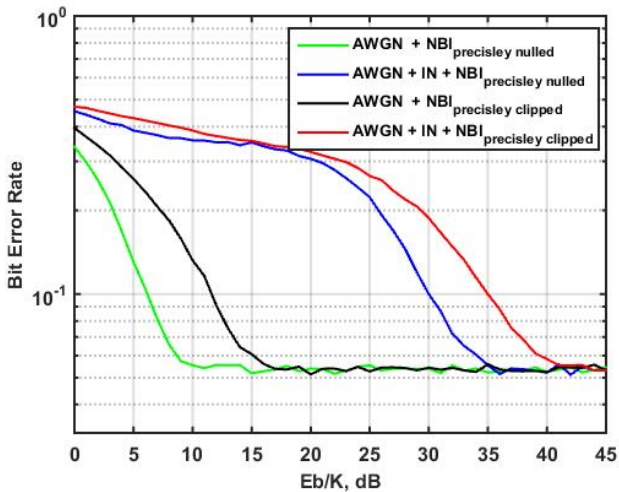Fig. 9. The comparison of MBPSK and QFSK clipping of NBI with an unmitigated conventional BPSK signal.

Fig. 8. The MBPSK scheme in cases of clipping and nulling NBI at perfect noise locations, where $\Lambda = \lambda = 0.25$, $\sigma_{nbi}^2 = 100$, $\Gamma = 0.01$, and $X = 0$.

the NBI was assumed to be identified perfectly, without the use of a threshold. Otherwise, threshold is later considered and discussed. Afterwards, to mitigate the effect of NBI, the amplitude of signal in the sub-carrier identified to be corrupted by NBI is to be either nulled or clipped to X the expected signal amplitude after every received block's element, R_l, in frequency domain has been compared against a threshold. If found to be greater than the threshold, it is considered corrupted by NBI therefore nulled or clipped. However, as already mentioned, by assuming perfect knowlwedge of NBI location, the NBI location amplitude will be nulled or clipped without considering the threshold. The NBI preprocessing results to a clipped vector, $\widehat{R}_l$ which is taken for demodulation. The simulation results of this operation are shown in Figures 5–8 for clipping and nulling NBI at perfect locations in frequency domain, for both QFSK and MBPSK. The clipping value was

set at $0.5 \times \sqrt{E_b}$. In Figure 5, QFSK, there are different error floors for nulling and for clipping. There is about 15dB performance difference between AWGN + NBI and AWGN + IN + NBI curves when $\Gamma = 0.1$. The difference changed to $\approx$ 25dB for $\Gamma = 0.01$ as also shown by Figures 7 and 8. Which means that the addition of IN in the NBI affected system worsens the performance by almost $10\log_{10}(1/\Gamma)$ when Γ is varied on the base 10. A similar relation is demonstrated in [11] where the effect of Γ is demonstrated based on the performance difference when varying Γ. On the contrary, MBPSK's performance does not differentiate between either nulling or clipping in terms of error floor whilst for QFSK, the error floor is higher when nulling than when clipping. The error floor suggests a certain level of failure of the system in identifying the correct signal, not NBI and a failure in correcting the error bit. To add, as shown by Figure 9, MBPSK suffers once NBI is preprocessed. The clipping of NBI in the presence of IN does not improve the system but introduces a floor. QFSK does need the NBI mitigation whilst MBPSK does not and still behaves better the non-clipped and clipped cases of QFSK.

V. CONCLUSION

The work presented in this paper has shown that modified BPSK-OFDM scheme outperforms QFSK-OFDM in dealing with the difficult problem of combatting the mixture of IN and NBI in a PLC channel. The analysis of the behaviour of each scheme in various cases was presented, showing how the IN and NBI affect the systems. From the results modified BPSK-OFDM outperforms QFSK-OFDM because of its better minimum distance. However, at higher SNR both schemes produce similar results when perfect detection of the individual noise types is emploed.

REFERENCES

[1] L. Lampe, *Power Line Communications: Principles, Standards and Applications from multimedia to smart grid.* John Wiley & Sons, 2016.

[2] L. G. de Oliveira, G. R. Colen, M. V. Ribeiro, and A. H. Vinck, "Narrowband interference error correction in coded ofdm-based plc systems," in *Proceddings of the 2016 IEEE International Symposium on Power Line Communications and its Applications (ISPLC)*, 2016, pp. 13–18.

[3] A. Vinck, F. Rouissi, T. Shongwe, G. R. Colen, and L. Oliveira, "Impulse noise and narrowband plc," *arXiv preprint arXiv:1509.07236*, 2015.

[4] S. V. Zhidkov, "Impulsive noise suppression in ofdm-based communication systems," *IEEE Transactions on Consumer Electronics*, vol. 49, no. 4, pp. 944–948, 2003.

[5] K. T. Ouahada, "Coded modulation for power-line communication channel," Ph.D. dissertation, University of Johannesburg, 2009.

[6] A. J. H. Vinck, "Coded modulation for powerline communications," *AEÜ International Journal of Electronics and Communications*, vol. 54, no. 1, pp. 45–49, Jan. 2000.

[7] T. Sanjana and M. Suma, "Combined nbi and impulsive noise cancellation in ofdm system," *International Journal of Advanced Information Science and Technology*, vol. 1, no. 2, Jun. 2012.

[8] D. Shrestha, A. Tonello, X. Mestre, and M. Payaró, "Simultaneous cancellation of narrow band interference and impulsive noise in plc systems," in *Proceeding of the 2016 IEEE International Conference on Smart Grid Communications (SmartGridComm)*, Sydney, NSW, Australia, Nov. 6-9 2016, pp. 326–331.

[9] Y. J., "Modelling, detection and mitigation of impulsive noise and narrowband interference for indoor broadband power line communication," Ph.D. dissertation, University of Liverpool, 2016.

[10] A. Bolaji and T. Shongwe, "BPSK-OFDM versus QFSK-OFDM in combating the effects of narrowband interference and impulsive noise in power line communication," in *Proceedings of the 2018 International Symposium on Communication Systems, Networks and Digital Signal Processing (CSNDSP)*, Budapest, Hungary, Jul. 18–20 2018, pp. 1–6.

[11] T. Shongwe, H. C. Ferreira, and A. Han Vinck, "Broadband and narrowband noise modeling in powerline communications," *Wiley Encyclopedia of Electrical and Electronics Engineering*, pp. 1–18, Dec 2015.

[12] T. Shongwe, V. N. Papilaya, and A. H. Vinck, "Narrow-band interference model for ofdm systems for powerline communications," in *Proceedings of the 2013 17th IEEE International Symposium on Power Line Communications and Its Applications (ISPLC)*, 2013, pp. 268–272.

[13] J. O. Smith, *Mathematics of the discrete Fourier transform (DFT): with audio applications.* Julius Smith, 2007.